3D reconstruction using a method of the planar homography from uncalibrated camera

Yong-In Yoon *, **Jong-Soo Choi** *, **Jun-sik Kwon**** , **Oh-Keun Kwon****
* Dept of Image Engineering, Chung-Ang University, 221 Heuksuk-dong Dongjak-ku, Seoul 156-756 Korea
Tel : +82-02-814-7444 Fax : +82-02-826-2505 E-mail: {yoonyi,jschoi}@imagelab.cau.ac.kr
**Dept of Electric Engineering, Semyung University, 21-1 Sinwol-dong Jecheon City, Chung-buk Province, 390-711 Korea
Tel : +82-43-649-1304 Fax : +82-02-826-2505 E-mail: {jskwon,kok1027}@semyung.ac.kr

Abstract: It is essential to calibrate a camera in order to recover 3-dimensional reconstruction from uncalibrated images. This paper proposes a new technique of the camera calibration using a homography between the planar patterns image taken by the camera, which is located at the three planar patterns image. Since the proposed method should be computed from the homography among the three planar patterns from a single image, it is implemented more easily and simply to recover 3D object than the conventional. Experimental results show the performances of the proposed method are the better than the conventional. We demonstrate the examples of 3D reconstruction using the proposed algorithm from image sequence.

Key Word: Camera Calibration, Homography, Planar Patterns, 3D Reconstruction

1. INTRODUCTION

When the digital image contents such as computer graphics, animations, the virtual reality and the games make a manufacture, it is easier to express 3-dimensional images in three dimensions for being implemented the virtual world. Therefore, a method of 3D reconstruction is widely applied to the fields of entertainment technology such as the augmented reality and 3D modeling [1][2][3].

A representation method of 3D image involves the rendering techniques exploiting computer graphics. Since the informations of an object surface are computed in details, the methods are generally taken a lot of time in order to make the modeling and rendering of 3D object. Unlike the methods, the techniques of image based rendering are recovered to the objects from the photographs taken by a calibrated camera [3]. These methods are available to the modeling and rendering of 3D objects of the real world in the objects fixed a shape such as a building, a box and the architecture. The object may be comparatively formed from a set of primitive and can be modeled and rendered to be used to a variety of primitive. Unfortunately, this method should allow a user to spend much time and effort to recover the object from the images. It is also impossible to represent the objects from natural scenes.

The methods to recover the objects from image sequence should be required auto-calibration from uncalibrated images. Auto-calibration is the process of determining internal camera parameters directly from multiple uncalibrated images. It is not easy to implement auto-calibration from image sequence. Therefore, the techniques of 3D reconstruction using auto-calibration involve considerable efforts to recover the objects from image sequence [4][5][6].

This paper proposes a new technique of a camera calibration to compute a homography between the planar patterns taken by a single image, which is located at the three planar patterns from uncalibrated images. Since the method of the camera calibration from uncalibrated images may generally happen to a problem to find correspondences between two images, it includes much more errors. The proposed method should be decreased the errors of the camera calibration from unclibrated images. We therefore used the technique to calibrate the camera from the images of the planar patterns. Zhang [7] proposed the camera calibration to exploit the homography among the images of the three planar patterns. This paper proposes the novel method to calibrate the camera using the homography between the planar patterns from a single image acquired with the camera, which is located at the three planar patterns from uncalibrated images. This method can be easily allowed a user to set up the coordinate system from the planar pattern images. Since the error elimination of 3-dimensional points should be used to a constrained condition, the proposed method to apply in the planar patterns can be diminished a lot of the errors in comparison with the conventional. The next step may be used to the matching informations between feature points of the planar patterns and computed to the fundamental matrix. If the epipole line is estimated, image rectification can be calculated. The final step should be computed to the correspondences of two images from a rectified image and can be easily implemented a system to recover 3D object by the back projection from 2D images.

This paper describes as follows. Section 2 presents the overall block diagram of the proposed algorithm, and explains a method to induce the intrinsic and extrinsic parameters of the proposed algorithm using camera perspective relationship and the planar pattern from projective space. Section 3 outlines a method to extract the fundamental matrix using correspondences of two planar patterns and describes the way of image rectification. Section 4 computes correspondences of images exploiting rectified image and presents the method to calculate 3D coordinates by the back projection and construction of disparity map. Section 5 shows the results of simulation for computing the errors of conventional algorithm and

proposed, and also demonstrates the examples of 3D reconstruction from uncalibrated images. Section 6 describes conclusions of this paper

2. THE PROPOSED ALGORITHM

2.1 The overall block diagram of the proposed algorithm

Figure 1 shows the overall block diagram of the proposed algorithm in this paper. First step extracts feature points for the planar patterns from uncalbrated images and draws in order of feature points for each planar patterns in the x and y direction respectively. The ordered feature points are computed to a homography of the image involved three planar patterns from a single image taken by each cameras and are calculated to the intrinsic and extrinsic parameters of the camera calibration by the homography. Second step estimates the fundamental matrix using the mapping information between feature points of these planar patterns. Since two cameras should be located on the straight line, it is necessary to rectify the images. Third step finds many matching points between right rectified image and left, and the dense disparity map may be constructed to look for all candidated correspondences of two images. The disparity map is easily computed to 3D coordinate points by the back projection. Finally, 3D coordinate points are constructed to a polyhedron by the Delauny Triangulation[17]. The polyhedron is implemented to 3D reconstruction by mapping its texture.

The proposed algorithm is used to two cameras and constructed to stereo cameras system to extract the depth information. The proposed system can be simply and easily implemented to 3D modeling for the image of object taken by the camera without the user input.

2.2 Camera Model

A camera is generally modeled by the usual pinhole: if a point $\mathbf{x}_i$ in the planar image coordinate system to correspond the point $\mathbf{X}_i$ on the 3D space is given, the relationship between two points should be satisfied with $x_i = P X_i$ for all points i to the 3×4 camera projection matrix.

$$\lambda_i \begin{bmatrix} x_i \\ y_i \\ 1 \end{bmatrix} = \begin{bmatrix} p_{11} & p_{12} & p_{13} & p_{14} \\ p_{21} & p_{22} & p_{23} & p_{24} \\ p_{31} & p_{32} & p_{33} & p_{34} \end{bmatrix} \begin{bmatrix} X_i \\ Y_i \\ Z_i \\ 1 \end{bmatrix} \quad (1)$$

The above projective matrix is 11 degrees of freedom. The following equation (2) is represented by the relationship between the original points of camera and the world coordinate system (3×3 is the rotional matrix R, 3×1 is the translation vector T).

$$P = K[R\ T] \quad (2)$$

$$K = \begin{bmatrix} f_x & s & o_x \\ 0 & f_y & o_y \\ 0 & 0 & 1 \end{bmatrix} \quad (3)$$

The intrinsic parameters **K** is an upper-trianglar matrix (3×3) involved 5 degree of freedoms. f_x and f_y are the scale factor in the x-coordinate and y-coordinate directions respectively. S is the skew. O_x and O_y denote the coordinate of the principal points [8].

2.3 The planar patterns and homography between the projective images

If we assume the horizontal and vertical for the planar patterns is the x and y axes of the world coordinate system and the normal direction of the planar patterns is the direction of the z axis such as Fig.2, the z coordinate for the planar patterns is 0. If the column of the rotation matrix R denotes r1, r2, r3, and the translation vector is T, the equation represents as follows.

$$s\begin{bmatrix} u \\ v \\ 1 \end{bmatrix} = K[r_1 \quad r_2 \quad r_3 \quad t]\begin{bmatrix} X \\ Y \\ 0 \\ 1 \end{bmatrix} = K[r_1 \quad r_2 \quad t]\begin{bmatrix} X \\ Y \\ 1 \end{bmatrix} \quad (4)$$

Therefore, a homography relationship between a point m into the image and the point M on the 3D coordinate system describes as follows.

$$sm = HM \text{ (where, } H = K[r_1 \quad r_2 \quad t]) \quad (5)$$

2.4 Extracting feature points

As the homography between the point of the world coordinate system and its image is computed, we should first find feature points for three planar patterns. This paper extracted the intersection of patterns in order to look for feature points and used the method of Harris corner detection [8]. This operator is as follows.

$$R(x, y) = \det[C] - k\,\mathrm{trace}^2[C] \quad (6)$$

$$C = \begin{bmatrix} I_x^2 & I_x I_y \\ I_x I_y & I_y^2 \end{bmatrix} \quad (7)$$

Here I_x and I_y denote the partial differential value of the x-axis and the y-axis directions respectively. k is constant and set up to o.o4 proposed by Harris' method. Since a noise happen to the wrong results, an input image is applied to the Gaussian filter and diminished an effect for the noise.

2.5 The algorithm of the proposed camera calibration

The proposed algorithm is derived from Zhang'[7]. Zhang' method used the homography among three planar patterns images. The proposed algorithm is acquired with a single image involved three planar patterns and is a new method exploited the relationship of homography into the image [9].

If the camera projection matrix $\mathbf{P} = \lambda \mathbf{K}[\mathbf{R}\,|\,\mathbf{t}]$ should be applied to the property of the rotation matrix $\mathbf{R} = [\mathbf{r}_1\ \mathbf{r}_2\ \mathbf{r}_3]$ from the equation (1) and (2), we denote the 3×3 sub-matrix as

$$\mathbf{H}_{\infty} = \lambda \mathbf{K}\mathbf{R} \quad (8)$$

Let us denote $\mathbf{H}_{\infty}$ and $\mathbf{R}$ as $\mathbf{H}_{\infty} = [\mathbf{h}_1\ \mathbf{h}_2\ \mathbf{h}_3]$ and $\mathbf{R} = [\mathbf{r}_1\ \mathbf{r}_2\ \mathbf{r}_3]$ respectively. From $\mathbf{K}^{-1}\mathbf{H}_{\infty} = \lambda\mathbf{R}$ and $\mathbf{H}_{\infty}^{T}\mathbf{K}^{-T} = \lambda\mathbf{R}^{T}$, we have

$$\mathbf{H}_{\infty}^{T}\mathbf{K}^{-T}\mathbf{K}^{-1}\mathbf{H}_{\infty} = \lambda^2\mathbf{R}^{T}\mathbf{R} = \lambda^2\mathbf{I} \quad (9)$$

The most left matrix can be written as follows:

$$\mathbf{H}_{\infty}^{T}\mathbf{K}^{-T}\mathbf{K}^{-1}\mathbf{H}_{\infty} = \begin{bmatrix} \mathbf{h}_1^{T}\mathbf{K}^{-T}\mathbf{K}^{-1}\mathbf{h}_1 & \mathbf{h}_1^{T}\mathbf{K}^{-T}\mathbf{K}^{-1}\mathbf{h}_2 & \mathbf{h}_1^{T}\mathbf{K}^{-T}\mathbf{K}^{-1}\mathbf{h}_3 \\ \mathbf{h}_2^{T}\mathbf{K}^{-T}\mathbf{K}^{-1}\mathbf{h}_1 & \mathbf{h}_2^{T}\mathbf{K}^{-T}\mathbf{K}^{-1}\mathbf{h}_2 & \mathbf{h}_2^{T}\mathbf{K}^{-T}\mathbf{K}^{-1}\mathbf{h}_3 \\ \mathbf{h}_3^{T}\mathbf{K}^{-T}\mathbf{K}^{-1}\mathbf{h}_1 & \mathbf{h}_3^{T}\mathbf{K}^{-T}\mathbf{K}^{-1}\mathbf{h}_2 & \mathbf{h}_3^{T}\mathbf{K}^{-T}\mathbf{K}^{-1}\mathbf{h}_3 \end{bmatrix} \quad (10)$$

It follows from the equation (9) and (10) that we have the following relationship.

$$\begin{bmatrix} \mathbf{h}_1^{T}\mathbf{K}^{-T}\mathbf{K}^{-1}\mathbf{h}_1 & \mathbf{h}_1^{T}\mathbf{K}^{-T}\mathbf{K}^{-1}\mathbf{h}_2 & \mathbf{h}_1^{T}\mathbf{K}^{-T}\mathbf{K}^{-1}\mathbf{h}_3 \\ \mathbf{h}_2^{T}\mathbf{K}^{-T}\mathbf{K}^{-1}\mathbf{h}_1 & \mathbf{h}_2^{T}\mathbf{K}^{-T}\mathbf{K}^{-1}\mathbf{h}_2 & \mathbf{h}_2^{T}\mathbf{K}^{-T}\mathbf{K}^{-1}\mathbf{h}_3 \\ \mathbf{h}_3^{T}\mathbf{K}^{-T}\mathbf{K}^{-1}\mathbf{h}_1 & \mathbf{h}_3^{T}\mathbf{K}^{-T}\mathbf{K}^{-1}\mathbf{h}_2 & \mathbf{h}_3^{T}\mathbf{K}^{-T}\mathbf{K}^{-1}\mathbf{h}_3 \end{bmatrix} = \lambda^2 \begin{bmatrix} 1 & 0 & 0 \\ 0 & 1 & 0 \\ 0 & 0 & 1 \end{bmatrix} \quad (11)$$

Under the condition (11), the linear equations on $\mathbf{K}^{-T}\mathbf{K}^{-1}$ are obtained as follows.

$$\begin{aligned} &\mathbf{h}_1^{T}\mathbf{K}^{-T}\mathbf{K}^{-1}\mathbf{h}_2 = \mathbf{h}_2^{T}\mathbf{K}^{-T}\mathbf{K}^{-1}\mathbf{h}_3 = \mathbf{h}_3^{T}\mathbf{K}^{-T}\mathbf{K}^{-1}\mathbf{h}_1 = \mathbf{0} \\ &\mathbf{h}_1^{T}\mathbf{K}^{-T}\mathbf{K}^{-1}\mathbf{h}_1 = \mathbf{h}_2^{T}\mathbf{K}^{-T}\mathbf{K}^{-1}\mathbf{h}_2 = \mathbf{h}_3^{T}\mathbf{K}^{-T}\mathbf{K}^{-1}\mathbf{h}_3 \end{aligned} \quad (12)$$

The matrix $\mathbf{K}^{-T}\mathbf{K}^{-1}$ can be considered as the conic coefficient matrix that has five degree of freedoms. A conic is determined uniquely (up to scale) by five points in general position [10]. From (12) we have six constraints being able to determine $\mathbf{K}^{-T}\mathbf{K}^{-1}$ using SVD [19].

Let us denote $\mathbf{Q}$ the matrix $\mathbf{K}^{-T}\mathbf{K}^{-1}$ calculated from the linear equations above, that is, $\mathbf{Q} = \mathbf{K}^{-T}\mathbf{K}^{-1}$ (up to scale). Hence we get $\mathbf{Q}^{-1} = \lambda\mathbf{K}\mathbf{K}^{T}$. Since $\mathbf{Q}^{-1}$ is symmetric, let us denote $\mathbf{Q}^{-1}$ as

$$\mathbf{Q}^{-1} = \begin{bmatrix} a_1 & a_2 & a_3 \\ a_2 & a_4 & a_5 \\ a_3 & a_5 & a_6 \end{bmatrix} \quad (13)$$

Then, from $\mathbf{Q}^{-1} = \lambda\mathbf{K}\mathbf{K}^{T}$, we have

$$\begin{bmatrix} a_1 & a_2 & a_3 \\ a_2 & a_4 & a_5 \\ a_3 & a_5 & a_6 \end{bmatrix} = \lambda \begin{bmatrix} f_x^2 + s^2 + o_x^2 & sf_y + o_x o_y & o_x \\ sf_y + o_x o_y & f_x^2 + o_y^2 & o_y \\ o_x & o_y & 1 \end{bmatrix} \quad (14)$$

Without difficulty, we can uniquely extract the intrinsic parameters from the equation (14). A solution of the equation (14) can be written as follows.

$$\lambda = a_6, o_x = a_3/a_6, o_y = a_5/a_6,$$

$$f_y = \sqrt{\frac{a_4 a_6 - a_5^2}{a_6^2}}, s = \left[\frac{a_2}{a_6} \frac{a_3 a_5}{a_6^2}\right] / f, f_x = \sqrt{\frac{a_1}{a_6} - s^2 - o_x^2} \quad (15)$$

Therefore, the rotation matrix and the translation are obtained by the equation using the relationship between the equation (8) and the camera matrix.

$$\mathbf{R} = \frac{1}{\det(\mathbf{K}^{-1}\mathbf{H}_{\infty})^{\frac{1}{3}}}\mathbf{K}^{-1}\mathbf{H}_{\infty},\ \mathbf{t} = \frac{1}{\det(\mathbf{K}^{-1}\mathbf{H}_{\infty})^{\frac{1}{3}}}\mathbf{K}^{-1}\mathbf{p}_4 \quad (16)$$

where $\mathbf{p}_4$ is the fourth column vector of $\mathbf{P} = \lambda\mathbf{K}[\mathbf{R}\,|\,\mathbf{t}]$. We note that the computed rotation matrix $\mathbf{R}$ can not satisfy with the property of the rotation matrix. Let the singular value decomposition of $\mathbf{R}$ be $\mathbf{U}\Sigma\mathbf{V}^{T}$, where $\Sigma = diag(\sigma_1, \sigma_2, \sigma_3)$. Since a pure rotation matrix has $\Sigma = diag(1,1,1)$, we set $\mathbf{R} = \mathbf{U}\mathbf{V}^{T}$ which is the best approximation matrix to the estimated rotation matrix [19].

3. THE FUNDAMENTAL MATRIX AND IMAGE RECTIFICATION

3.1 Estimation of the Fundamental Matrix

As shown in Fig 3, if a point M of the world coordinate system is projected by C_1, C_2 through two cameras and the coordinate points mapped to each images are considered the image points m_1 and m_2, the image points m_1 and m_2 are related by the correspondences. The fundamental matrix F of C_2 for C_1 of reference camera can be written as follows [10] [15].

$$l_{m1} = \mathrm{F}\,\tilde{m}_1 \quad (17)$$

$$\tilde{m}^{T}{}_2\,\mathrm{F}\,\tilde{m}_1 = 0 \quad (18)$$

$$F\tilde{e}_1 = \mathrm{F}^{T}\tilde{e}_2 = 0 \quad (19)$$

where l_{m1} denotes the epipolar line of the point m_1 to the right image for the left image, e_1 and e_2 are the epipole, intersection connected the center of two cameras. The plane of M, C_1, and C_2 is called the epipolar plane. All points of l_{m2} for the left image include the points of l_{m1} for the right image.

This paper used the method of RANSAC in order to compute the fundamental matrix [16].Subheadings are in bold letters and placed flush on the left-hand margin of the column.

3.2 Image Rectification

If an image is rectified, a matching problem of two images can be solved much more effectively. Image rectification consists of transforming the images so that the epipolar lines are aligned horizontally. If the rectified image should be built up, the stereo matching problem allows the searching area to reduce by one dimension. The conventional method consists of transforming to the image of a single plane for 3D space of two images [11] [12] [13]. This paper used the method transforming a polar coordinate system exploiting the epipole, the polar coordinate of an length and an angle in the x and y reference coordinate system of the image [14]. For a case the polar coordinate system using the angle transforms, the unnecessary pixels for the angle may take place. Therefore, if the polar coordinate system of the angle transforms, the y reference coordinate system to the opposite direction of the epipole in the image is used. This transformation is a method that the unnecessary pixels do not happen. The polar coordinate system also may be transformed differently in comparison with image rectification using a homography. Consequently, in case the epipole located into the image, the method that we used allows the rectified image to be eliminated to overpass infinitely.

4. CONSTRUCTION OF DISPARITY MAP

A case that construction of disparity map for 3D

modeling in the stereo images is ideal find all correspondences of the two images and is that a dense disparity map is built up. It is a disparity map that is the most difficult part in the image based modeling. The disparity map depends upon results of final modeling. The cases constructed the disparity map are two methods: one finds interpolation of viewpoint, the other extracts correspondences by the back projection for 3D reconstruction[18]. It is important for interpolation of viewpoint to build up the dense disparity map. Since the disparity map of 3D reconstruction however forms the type of a polygon for a set of projective 3D points, the accurate disparity map is much more important.

This paper first minimizes a generating ratio of error and sets up a window of a definite size for the pixels of each image in the construction of 3D modeling. The pixels of the images are computed a variance of the window into the image. The pixels over the threshold of the variance into the window then are extracted from the candidated points among all correspondences. The disparity map is formed by the candidated points.

$$Var(m_1,m_2)=\frac{\sum_{i=-n}^{n}\sum_{j=-m}^{m}[I_1(u_1+i,v_1+j)-\overline{I_1(u_1,v_1)}]}{(2n+1)(2m+1)} \quad (20)$$

(where, $\overline{I_k(u,v)}=\sum_{i=-n}^{n}\sum_{j=-m}^{m}I_k(u+i,v+j)/[(2n+1)(2m+1)]$)

5. EXPERIMENTAL RESULTS

5.1 Extraction and ordering for feature points of the pattern image

In order to calibrate a camera, this paper uses two cameras and takes a single image located at the three planar patterns from uncalibrated images and then simulates to the input images. Fig. 4 and Fig. 5 are the input images. An operator of Harris corner detection may be first used to extract feature points of a pattern image and ordered to input image for four points of each pattern edges. Fig.6. shows the images extracted feature points from the pattern image for the right and left image. Feature points is a preprocess work for computing a homography among the three planar patterns. To easily find feature points, this paper exploited the planar patterns image. Feature points to be detected from Fig.6 are calculated and therefore Fig.7 represents the ordered feature points. After the homography between the images to be set up by the ordered feature points is estimated, the camera calibration is obtained. A 3D coordinates point to be built up is computed and then constructed by the projective matrix from the intrinsic and extrinsic parameters. Zhang' method as well as the proposed algorithm is applied to simulation.

5.2 Computation of the intrinsic and extrinsic parameters from a pattern image

Table 1 represents the experimental results for the intrinsic and extrinsic parameters of a camera computed the proposed algorithm from the input images of Fig. 4, Fig. 5.

The rotation matrix **R** is components of R_1, R_2, R_3. The translation matrix denotes a vector of translation distance for a right and left of the camera. The intrinsic parameters K are also the matrix of 3X3. We here assume the skew is 1.

The simulation of the camera calibration for the proposed algorithm and Zhang' method is compared with the generated error to recover 3D coordinate points from sample images. The typical sample images are Fig.8. Sample images are a representative out of 50 images. Comparing objects are the images to calibrate the camera from sample images. Each vertexes of recovering objects is ordered to A, B, C ... G. As a size of a line segment is assumed to 1, a linked length between the vertexes can be compared with the errors. As shown in Fig.10, let us consider a line segment AB connecting the vertex A and the vertex B, the line segment CD connecting the vertex C and the vertex D, the line segment EF connecting the vertex E and the vertex F, the line segment BD connecting the vertex B and the vertex D, the line segment AC connecting the vertex A and the vertex C, the line segment GE connecting the vertex G and the vertex E, the line segment DF connecting the vertex D and the vertex F, the line segment CE connecting the vertex C and the vertex E, and the line segment AG connecting the vertex A and the vertex G. The errors of a length ratio for AB:CD:EF, BD:AC:GE and DF:CE:AG are recovered 3D coordinate points from sample images and computed. Table 2 shows an average value of RMS error for 50 images is calculated. The proposed algorithm for AB:CD:EF, BD:AC:GE and DF:CE:AG is that the average values of RMS error are 0.023,0.025, and 0.027 respectively. The conventional algorithm for the average values of RMS error is 0.029, 0.03, and 0.033 respectively. We can know that the proposed algorithm is better than the conventional.

Since sample images are also the rectangular image, these can be computed to the errors of being happened the rectangular angle to recover 3D coordinate points from images. Let us consider the angle 1 as the angle CAB, the angle 2 as the angle ABD, the angle 3 as the angle CDB, the angle 4 as the angle ACD, the angle 5 as the angle ECD, the angle 6 as the angle CDF, the angle 7 as the angle EFD, the angle 8 as the angle ACD, the angle 9 as the angle GAC, the angle 10 as the angle AGE, and the angle 11 as the angle GEC. Table 3 shows the value of the error for the rectangular angle. The value of the error for the angle 11 is used to the RMS. The conventional method is 6.37 and the proposed is 2.38. In comparison with the errors for the angle, we can know that the proposed algorithm is better than the conventional. Table 4 represents the results calculated the fundamental matrix and the epipole from the doll image of Fig 4 and Fig 5. The fundamental matrix should be used to compute image rectification.

5.3 The experiments for image rectification and the disparity map

The fundamental matrix and the epipole are estimated from two images. As shown in Table 4, image rectification consists of transforming the images so that the epipolar lines are aligned horizontally. Fig.9 represents image rectification transformed to compute the epipolar lines horizontally between a right image and a left. Fig.10 shows a rectified image of the right and the left. An accurate matching from the rectified image should be implemented. Fig.11 denotes the results estimated the matching candidates by the variance value. This is the

disparity between the right and the left images. After the disparity map is therefore constructed by an edge from the rectified image of the right and the left, a distribution of the computed disparity is shown in Table 5. Table 5 describes the distribution chart of the disparity that the disparity map is accurately computed and built up the matching candidates. In this paper, the disparity map below the threshold of the average value is eliminated by the errors. Table 5 represents the disparity map ranges from 108 to 156.

5.4 Implementation of 3D reconstruction

The estimated 3D points can be projected by the back projection. 3D coordinate points computed by the back projection can be then formed to a polygon by the Delaunay triangulation. Fig. 12 shows reconstruction of 3D points by the back projection and computed 3D points from input images. Fig. 13 denotes the polygon constructed by 3D points. Fig. 14 represents the image implemented 3D points by OpenGL.

6. CONCLUSIONS

In this paper, a camera calibration exploiting the planar pattern from uncalibrated images should be used to the planar homography and proposed a new method of the camera calibration. Experimental results demonstrated the performance of the proposed algorithm is better than one of the conventional.

As the camera calibration, the fundamental matrix, the disparity map, and the back projection are simulated in the case of image based modeling, the errors happen to all part of 3D reconstruction system. Image based modeling finally involved a lot of difficulties. This paper therefore used the camera calibration from the planar patterns image in order to minimize the errors. It is possible to calibrate the camera taken by a single image of the three patterns. A method of MLE (Maximum Likelihood Estimation) is applied to extract the parameters of the optimized camera. As the fundamental matrix used to image rectification was computed, the errors are minimized to use the method of RANSAC. After the disparity map was extracted from the candidates of correspondences, it was detected to the correlation between two images and constructed. If the distribution of the disparity map was calculated, the disparity below the threshold was removed to correspondences involved the errors. Like this course, an object allows a user to implement 3D reconstruction system.

7. ACKNOWLEDGMENT

This research was supported by the Ministry of Education, Seoul, Korea, under the BK21 project, and by the Ministry of Science and Technology, Seoul, Korea, under the NRL project.

REFERENCE

[1] R. T. Azuma, "A Survey of Augmented Reality", Presence: Teleoperators and Virtual Environments, vol. 6, no. 4, pp. 355-385, 1997.

[2] Y. Ohta and H. Tamura, "Mixed Reality-Merging Real and Virtual Worlds", Ohmsha Ltd. & Springer-Verlag, 1999.

[3] R P.E Deebevec, C.J Taylor, and J. Mailk, "Modeling and Rendering Architecture from Photographs: A Hybrid Geometry and Image-Based Approach", In Proceedings of ACM SIGGRAPH 1996, ACM Press / ACM SIGGRAPH, pp.11-21, Aug. 1996

[4] P.Beardsley,P.Torr and A.Zisserman, "3D Model Acquisition from Extended Image Sequences", In Proceeding 4th European Coference on Computer Vision, Cambridge, LNCS 1065, Volume II, page 683-695, Springer-Verlag, 1996

[5] M. Pollefeys, R. Koch and L. Van Gool, "Self-Calibration and Metric Reconstruction in spite of Varying and Unknown Internal Camera Parameters", International Journal of Computer Vision, 32(1), 7-25, 1999.

[6] C.Tomasi and T. Kanade, "Shape and motion from image streams under orthography: a factorization method", International Journal of Computer Vision, 9(2), 137-154, 1990.

[7] Zhengyou Zhang, "A Flexible New Techinque for Camera Calibration", IEEE Transaction on Pattern Analysis and Machine Intelligence, vol.22, no.11, pp.1-20, 2000.

[8] C. Harris and M. Stephens, "A combined corner and edge detector", Fourth Alvey Vision Conference, pp.147-151, 1988

[9] Jang-Hwan Im, Yong-In Yoon, and Jong-Soo Choi, "A linear method for camera calibration and its application to augmented reality", 6th ACCV, Jan. 2004, pp.617-621.

[10] R. Hartely and A. Zissermann, "Multiple View Geometry in Computer Vision", Cambridge University Press, 2000.

[11] O. Faugeras, "Three-Dimensional Computer Vision: a Geometric Viewpoint", MIT press, 1993.

[12] N. Ayache and C. Hansen, "Rectification of images for binocular and trinocular stereovision", Proc. International Conference on Pattern Recognition, pp. 11-16, 1988.

[13] D. Papadimitriou and T. Dennis, "Epipolar line estimation and rectification for stereo image pairs", IEEE Trans. Image Processing, 5(4):672-676, 1996.

[14] Pollefeys, M. Koch, R. Van Gool, L. "A simple and efficient rectification method for general motion", Proc.ICCV pp.496-501, Corfu (Greece), 1999.

[15] R. Deriche, Z. Zhang, Q.-T. Luong and O. Faugeras, "Robust Recovery of the Epipolar Geometry for an Uncalibrated Stereo Rig", European Conference on computer Vision, Vol.1, pp. 567-576, Stockhom, Sweden, May 1994.

[16] M. Fischler and R. Mourrain, "RANdom SAmpling Consensus: a paradigm for model fitting with application to image analysis and automated cartography", Commun. Assoc. Comp. Mach., 24:381-95, 1981.

[17] Mark de Berg, Marc van Kreveld, Mark Overmars, and Otfried Schwarzkopf, "Computational Geometry: Algorithms and Applications", second edition, Springer-Verlag, 2000.

[18] Y. Shan and Z. Zhang, "New Measurements and Corner-Guidance for Curve Matching with Probabilistic Relaxation", International Journal of Computer Vision, vol.46, no.2 pp.157-171, 2002.

[19] G. Golub and C. van Loan, "Matrix Computations", The John Hopkins University, Baltimore, Maryland, 3 edition, 1996.

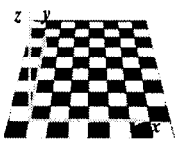

Fig.2. The coordinate system of the planar patterns

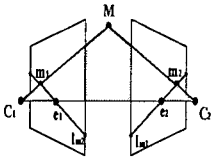

Fig 3. Epipola geometry

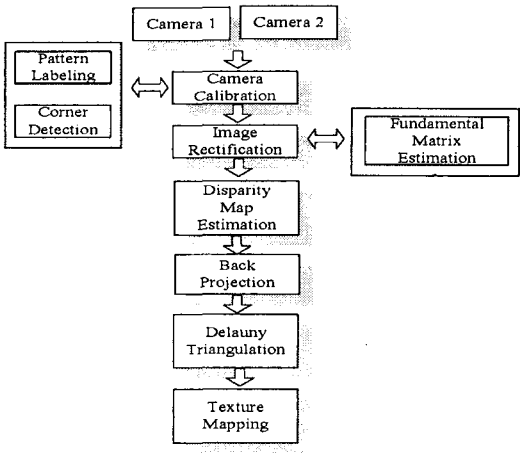

Fig.1. The overall block diagram of the proposed algorithm.

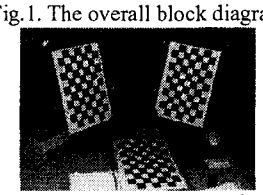

Fig.4. An input image of a left doll

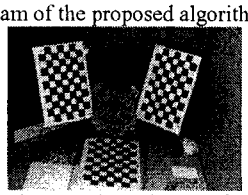

Fig.5. An input image of a right doll

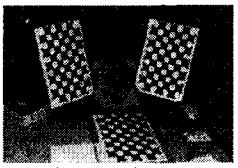

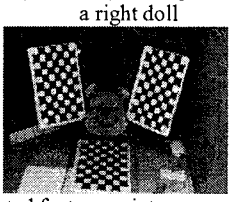

Fig.6. An image extracted feature points

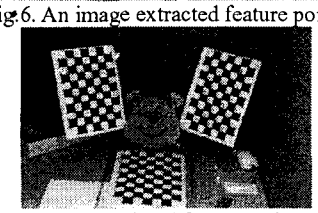

Fig.7. A ordered feature points

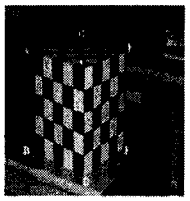

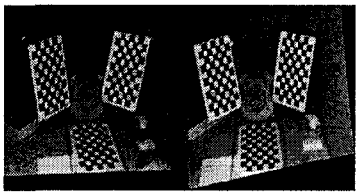

Fig.8. A sample image Fig.9. Image rectification

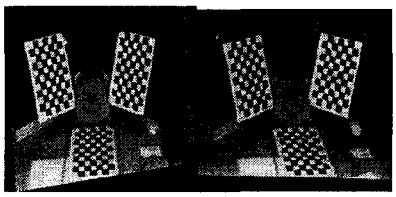

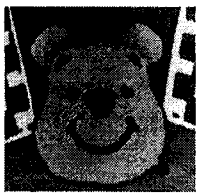

Fig.10. A rectified image Fig.11

<Fig.11.The matching candidates based on the variance value>

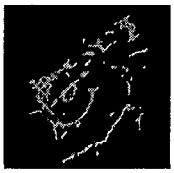

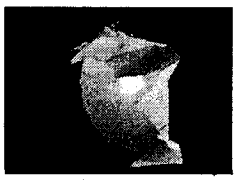

Fig. 12 Fig. 13 Fig.14

<Fig 12. Reconstruction of 3D points>
<Fig.13. A polygon for 3D points>
<Fig.14. 3D reconstruction implemented by the OpenGL>

Input image	The doll image(left)		
Rotation components	0.998886	0.040753	-0.023772
	0.998886	-0.746565	-0.665152
	-0.044854	0.664063	-0.74633
Translation components	-76.74468	172.577577	539.28478
Intrinsic parameters	Ox	513.733589	
	Oy	373.094744	
	fx	1198.148237	
	fy	1193.746485	
Input image	The doll image(right)		
Rotation components	0.998883	-0.007386	0.046675
	0.025065	-0.754518	-0.655801
	0.040062	0.656238	-0.75349
Translation components	-25.082835	184.042526	525.1303 5
Intrinsic parameters	Ox	472.984713	
	Oy	343.197327	
	fx	1214.748703	
	fy	1207.029158	

Table 1. Computation for the intrinsic and extrinsic parameters of a camera using the proposed algorithm

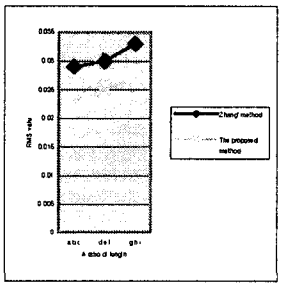

Table 2.

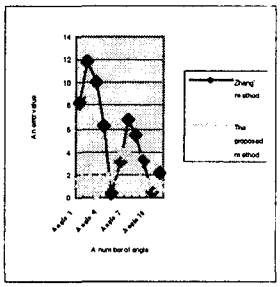

Table 3

<Table 2. Comparison for a ratio of length>
<Table 3. Comparison of the errors for the rectangular angle>

The funmamental matrix	2.49734E-06	-3.3507E-06	0.000775527
	-8.08592E-06	2.53161E-07	-0.0753111
	-0.006025611	0.08178137	1
The left epipole	-9308.660069	-698.085259	1
The right epipole	23304.53116	253.2602136	1

Table 4. The doll image of the fundamental matrix and the epipole

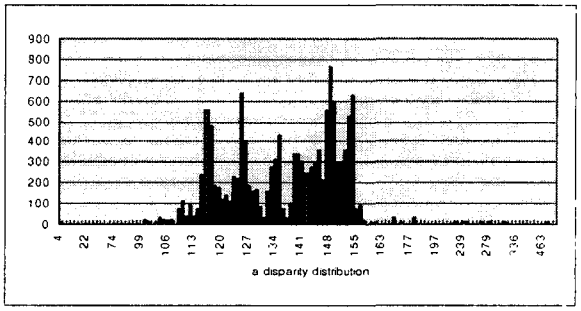

Table 5. A distribution chart of an estimated disparity